View metadata, citation and similar papers at core.ac.uk
brought to you by CORE
provided by DSpace@MIT

Improved Performance of High Areal Density Indirect Drive Implosions at the National Ignition Facility using a Four-Shock Adiabat Shaped Drive

D. T. Casey,[1] J. L. Milovich,[1] V. A. Smalyuk,[1] D. S. Clark,[1] H. F. Robey,[1] A. Pak,[1] A. G. MacPhee,[1] K. L. Baker,[1] C. R. Weber,[1] T. Ma,[1] H.-S. Park,[1] T. Döppner,[1] D. A. Callahan,[1] S. W. Haan,[1] P. K. Patel,[1] J. L. Peterson,[1] D. Hoover,[2] A. Nikroo,[2] C. B. Yeamans,[1] F. E. Merrill,[3] P. L. Volegov,[3] D. N. Fittinghoff,[3] G. P. Grim,[3] M. J. Edwards,[1] O. L. Landen,[1] K. N. Lafortune,[1] B. J. MacGowan,[1] C. C. Widmayer,[1] D. B. Sayre,[1] R. Hatarik,[1] E. J. Bond,[1] S. R. Nagel,[1] L. R. Benedetti,[1] N. Izumi,[1] S. Khan,[1] B. Bachmann,[1] B. K. Spears,[1] C. J. Cerjan,[1] M. Gatu Johnson,[4] and J. A. Frenje[4]

[1]*Lawrence Livermore National Laboratory, Livermore, California 94550, USA*
[2]*General Atomics, San Diego, California 92121, USA*
[3]*Los Alamos National Laboratory, Los Alamos, New Mexico 87545, USA*
[4]*Massachusetts Institute of Technology, Cambridge, Massachusetts 02139, USA*

(Received 22 April 2015; published 1 September 2015)

Hydrodynamic instabilities can cause capsule defects and other perturbations to grow and degrade implosion performance in ignition experiments at the National Ignition Facility (NIF). Here, we show the first experimental demonstration that a strong unsupported first shock in indirect drive implosions at the NIF reduces ablation front instability growth leading to a 3 to 10 times higher yield with fuel $\rho R > 1$ g/cm^2. This work shows the importance of ablation front instability growth during the National Ignition Campaign and may provide a path to improved performance at the high compression necessary for ignition.

DOI: 10.1103/PhysRevLett.115.105001 PACS numbers: 52.57.Fg

In inertial confinement fusion (ICF) experiments performed at the National Ignition Facility (NIF) [1], capsules of deuterium and tritium fuel are imploded to high densities and temperatures to initiate alpha-particle self-heating and fusion burn [2,3]. The indirect drive ICF concept uses a laser to irradiate a high-Z cylindrical hohlraum, which produces a nearly uniform, thermal, x-ray drive. The x-ray drive then ablates an outer capsule shell imploding the remaining cryogenically frozen DT shell-mass inward. To achieve ignition, the DT hot spot must have high enough energy-density confined for adequate time to spark hot spot self-heating and start a burn wave through the dense DT shell. This requirement can be equivalently expressed as a condition of $P\tau$, where P is the hot spot pressure, a measure of the energy density, and τ is the confinement time of that energy [4]. It has been shown [5] that P is related to the implosion velocity (v) by balancing the hotpot internal energy to the shell kinetic energy via $2\pi PR^3 \sim \epsilon \frac{1}{2} M v^2$, where R is the radius of the hot spot, ϵ is the fraction of the shell kinetic energy converted to hot spot energy, and M is the mass of the shell. The hot spot confinement time is related to the shell inertia as $\tau \sim \sqrt{M/4\pi PR}$, and combining with the previous expression shows that $P\tau \sim \epsilon^{1/2} v\rho R$ [5], where ρR is the areal density. This means that a successful ignition experiment must simultaneously achieve efficient coupling of the shell kinetic energy to the hot spot, high v, and high ρR.

Achieving high implosion v and high ρR is challenging as the implosion process is subject to the Rayleigh-Taylor (RT) instability [6–8], which becomes more virulent with the higher accelerations required to get high v and with the steeper density gradients and higher convergences inherent for higher ρR. Experiments during the National Ignition Campaign (NIC) [9–13] were thought to have been degraded by both instability growth and in the most severe cases mix of plastic ablator material into the hot spot as a consequence of that growth. Subsequent experiments deliberately increased the adiabat (α) or entropy delivered to the DT shell, by increasing the laser foot (called high foot) to improve stability and performance [14–16]. Here, α is defined as $\alpha = P/P_{\text{cold}}$, where P_{cold} is the minimum pressure at 1000 g/cc from the DT EOS [17]. Increasing the α is one path to reduced ablation front hydrodynamic instability growth, and a hypothesis is that the reduced growth [18] led directly to improved performance demonstrated by the high-foot experiments [16]. The increased α is also predicted to lead to lower convergence, ρR, and yields in 1D simulations. In turn, reduced convergence leads to both reduced RT and Bell-Plesset growth [19] of instabilities at the ice-ablator interface and the ice-gas interface and a reduction in their perturbative impact even for fixed final amplitude. Additionally, Dittrich *et al.* [14] hypothesized that an increased foot level would reduce the ablation front physics sensitivity to uncertainties in the partially ionized ablated carbon. These multiple hypotheses left the role of ablation front growth during the NIC ambiguous.

To address the role of ablation front growth, a new laser pulse was designed by Milovich *et al.* [20] to produce the radiation drive proposed by Clark *et al.* [21] aimed at

 © 2015 American Physical Society

combining the best features of both the high ρR low-foot (LF) and improved stability high-foot (HF) drives. This new laser pulse shape launches a stronger first shock using a higher energy picket [see Fig. 1(a)] but with a standard low-foot trough so that the first shock decays as it traverses the ablator, weakening to comparable velocity to the LF implosion when it hits the DT ice, thus maintaining a low fuel adiabat [23]. The longer picket in this new "adiabat-shaping" (AS) pulse launches a first shock similar to that of HF, but with lower laser power and lower risk of laser-plasma instabilities during the picket. The approach is similar to the AS [24–28] techniques previously fielded in direct drive implosions [29–31]. In this case, however, the stability benefits are a consequence of the Richtmyer-Meshkov (RM) oscillations [32–35] during the shock transit phase, rather than a reduction of the RT growth rate directly [21]. That is, the ablation front RM oscillation occurs faster with the higher picket, moving the node in the growth factor spectrum to lower mode numbers, reducing the peak growth amplitude [see Fig. 1(b)]. X-ray radiography measurements of imposed sinusoidal modulations confirmed [36] that indeed the peak ablation front growth factor was reduced by moving an RM node closer to the peak of the RT growth factor using this drive as predicted by Clark *et al.* [21].

In this Letter, we show for the first time that this new pulse shape leads to significantly higher implosion performance at high ρR. These results suggest a dominant role of ablation front growth as a degradation mechanism of implosion performance during the NIC (even without the observation of ablator mix). This is accomplished by changing the ablation front growth characteristics, while achieving the same convergence and areal density. More importantly, these results may provide a viable path toward high performance implosions at the high areal densities required for ignition.

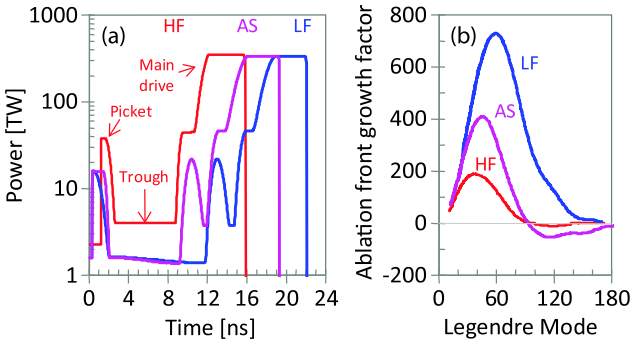

FIG. 1 (color online). (a) Laser pulse shape for the low adiabat or low foot (blue curve), the high adiabat or high foot (red), and the adiabat shaped (purple) drives. The high-power feature for the first ~3 ns is called the picket, and the trough is the following segment at low power. Features following the trough launch additional shocks, three shocks total for HF, and four shocks total for AS and LF. (b) Ablation front growth factors for the LF (blue), AS (purple), and HF (red) simulated using the code HYDRA [22].

A similar concept derived from the three-shock HF platform was to lower the trough below that of the LF pulse [37], allowing the first shock to weaken before it hits the DT ice [23], modestly reducing the adiabat (~10%). The details and results of this three-shock AS are described by Smalyuk *et al.* [38]. However, the three-shock AS represents a relatively small change in adiabat from the HF design, while the four-shock AS results described herein (at significantly lower adiabat than HF) are derived from the LF platform and therefore can be more directly related to the performance of the NIC. It is also possible, in principle, to achieve higher ρR, higher hot spot pressure, and higher simulated 1D performance, with this four-shock AS design [21].

The experiments described herein use the nominal ignition hohlraum and capsule design described in detail in Ref. [17]. The hohlraums were 5.75 mm in diameter with a depleted uranium (DU) wall overcoated with ~0.5 μm of Au [39,40]. A 69 ± 1.2 μm thick DT layer was cryogenically frozen on the inner surface of the capsules. The capsules were CH plastic nominally 1.1 mm in outer radius and 195 μm thick. The capsules were doped with graded Si at 1%, 2%, 1% (1 × Si) or 2%, 4%, 2% (2 × Si) at locations described in Ref. [12] (see Table I). The Si dopant shields the ice-ablator interface from hard x rays that can preheat this interface producing an unfavorable Atwood number leading to increased classical RT growth. However, increased dopant concentration also steepens the ablation front density gradient leading to more ablation front growth. The graded dopant configuration is designed to optimize these trade-offs [43]. Simulations predict that 2 × Si is more stable to interface growth while more unstable to ablation front growth. The capsule is supported inside the hohlraum with a thin membrane or "tent." The LF experiments discussed below can be considered nominally the same with the differences highlighted in Table I. One notable difference is the AS experiment uses a thinner tent than the LF implosions which is expected to reduce a seed for ablation front instability growth [44]. Another notable difference in the comparison with the HF drive is that the rate of rise of the main drive is steeper with a 2 ns duration rather than the 3 ns for the AS and the LF shots discussed herein. This steeper drive can result in higher velocities and may also have some RT consequences.

The main differences highlighted in this Letter concern the laser pulse shapes used to drive the hohlraum. Figure 1 shows three pulse shapes designed to achieve comparable peak implosion velocity at similar laser energies but with different fuel α and stability properties [20,21]. The four-shock LF pulse shape was designed to achieve low fuel α (~1.5), and on shot N120321 this drive demonstrated the highest observed ρR [45] and experimental ignition threshold factor [ITFX $= (Y/3 \times 10^{15}) \times (\rho R/1.5)^{2.3} \sim 0.1$]

TABLE I. Summary of performance parameters between comparable LF, HF, and AS shots [41,42].

	N141123	N120311	N120321	N120316	N120417	N120626	N130812
Laser energy [MJ], hohlraum	1.60, DU	1.58, DU	1.57, DU	1.56, DU	1.67, Au	1.70, Au	1.69, Au
Pulse	AS	LF	LF	LF	LF	LF	HF
Peak power (Au eq.) [TW]	339 (361)	334 (359)	332 (357)	330 (355)	(355)	(374)	(355)
Rise duration [ns]	3	3	3	3	3	3	2
Dopant	$1\times$ Si	$1\times$ Si	$2\times$ Si	$2\times$ Si + Ge	$2\times$ Si	$2\times$ Si	$1\times$ Si
Capsule tent thickness [nm]	31	112	110	110	110	110	44
Velocity [km/s]	320 ± 20	318 ± 20	321 ± 20	316 ± 20	314 ± 20	314 ± 20	333 ± 20
Total yield [10^{14}]	13.67 ± 0.23	1.59 ± 0.05	5.36 ± 0.18	2.75 ± 0.08	5.32 ± 0.13	1.18 ± 0.03	27.85 ± 0.59
Ti [keV]	3.4 ± 0.15	1.95 ± 0.24	3.14 ± 0.4	2.41 ± 0.25	3.05 ± 0.4	1.80 ± 0.14	4.02 ± 0.2
DSR [%]	5.45 ± 0.19	4.97 ± 0.3	6.24 ± 0.6	5.8 ± 0.32	5.32 ± 0.2	4.55 ± 0.22	3.96 ± 0.2
Hot spot radius [μm]	24.8 ± 2.5	25.5 ± 3.3	24.2 ± 2.6	25.6 ± 2.5	24.3 ± 1.9	31.5 ± 2.9	36.8 ± 2.6
$P\tau$ [atm*s]	16.4 ± 2.1	12.5 ± 4.4	13.3 ± 3.3	10.9 ± 2.7	11.6 ± 3.3	7.6 ± 2.0	14.2 ± 1.8

during the NIC [12]. Additionally, N120321 had four closely related companion shots summarized in Table I. Shot N130812 utilized the three-shock HF pulse shape, designed for higher fuel α (2.3–2.7) to improve the stability, and reduce the convergence ratio [14]. Shot N141123 used the four-shock AS pulse shape discussed here, designed to improve the stability properties while maintaining low fuel adiabat [$\alpha\sim1.6$]. This drive was designed to closely resemble the five LF companions (see Table I) only with reduced instability growth via increased energy in the picket. The power level of the picket was kept the same as the LF to maintain similar levels of early cross-beam-energy transfer [46], but with increased picket duration to provide higher picket drive temperature and initial shock strength [20]. Note that the actual delivered laser energy for N141123 was 8% lower in the picket than requested, which simulations predict increased the peak growth factor by ~1.6×. To account for this, the curves in Fig. 1(b) are from post-shot calculations for the actual delivered drives. It is also noteworthy that another drive has been designed with slightly more requested picket energy [23], which is predicted to result in further reduced growth at comparable adiabat.

The primary and down-scattered neutron images [47] from the neutron imaging system (NIS) are shown in Fig. 2 for the AS (a), LF (b), and HF (c) implosions. The primary 13–17 MeV neutron contours [48] (red) are formed by DT neutrons escaping from the core, while the down-scattered contours (black) are lower energy neutrons (6–12 MeV) resulting from DT neutrons scattering off the stagnated mass assembly. The NIS images suggest the AS implosion shows comparable shell shape and size to the LF, while the hot spot is roughly the same size but more oblate. The HF implosion N130812 on the other hand, shows a ~40% larger shell (consistent with a ~30% lower ρR) and a strong toroidal shaped hot spot [15]. The measured yield of unscattered neutrons is obtained by the activation of Zr using the flange nuclear activation detectors (FNADs) [49], which is sensitive to the $\Delta\rho R$ along multiple lines of sight. The FNADs data for the AS and LF show lower activation on one or both poles, consistent with increased shell ρR in these directions. These ρR asymmetries are hypothesized to be a consequence of polar jets formed by low mode (2–4) asymmetries [50] from this intrinsic hohlraum-beam geometry and may be further impacted by perturbations from the tent. These asymmetries are also thought to reduce the coupling efficiency of the shell to the hot spot [51] and strongly degrade the yield compared to 1D predictions, an active area of research where mitigation strategies are currently being developed.

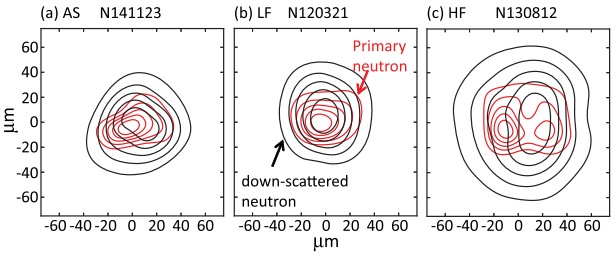

FIG. 2 (color online). (a)–(c) Neutron images obtained using the Neutron Imaging System [47] of (a) AS shot N141123, (b) LF N120321, and (c) HF N130812.

Figure 3 shows the total neutron yield as a function of average fuel ρR [12,52–54] for the AS (purple square), LF (blue), and HF (red) implosions. Also included are all LF NIC implosions (gray squares) beyond the five companions in Table I. The AS shot achieved comparable fuel ρR to the LF, consistent with the comparable in-flight adiabat inferred from shock velocity measurements [23]. However, the measured neutron yield of the AS implosion N141123 was considerably higher than all of the LF shots and 3–10 times higher than the closest companion shots (blue squares). Also shown is the HF implosion N130812. Despite the higher total yield of the HF, both the AS and HF shots lie on contours of ~1.5× yield amplification due to the dependence of α-particle self-heating on hot spot ρR, which is inferred to be higher due to the higher DSR [55] achieved with the AS drive.

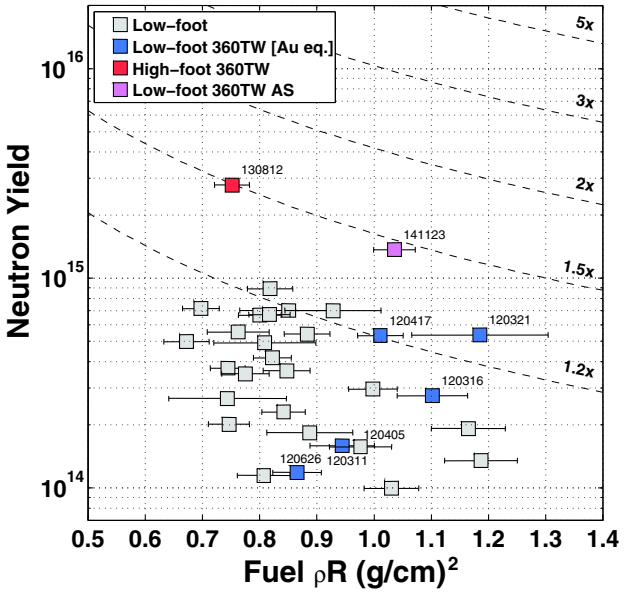

FIG. 3 (color online). Total neutron yield plotted as a function of fuel ρR for the AS, HF, and LF implosions. The dashed curves are contours of calculated yield amplification from hot spot alpha self-heating. The AS achieved significantly higher yield than the LF platform at comparable ρR.

The measured neutron yield is plotted as a function of the inferred CH ablator mix mass in the hot spot in Fig. 4(a). The CH mix mass is inferred from the hard x-ray yield to neutron yield ratio because of its dependence on hot spot effective Z [11,12]. This plot shows that for implosions with inferred CH mix mass >100 ng (the approximate threshold for detection), the measured yields are low ($<4 \times 10^{14}$). This is likely due to a failure of the integrity of the DT shell along with increased radiative energy loss from the injection of higher-Z CH(Si) in the hot spot.

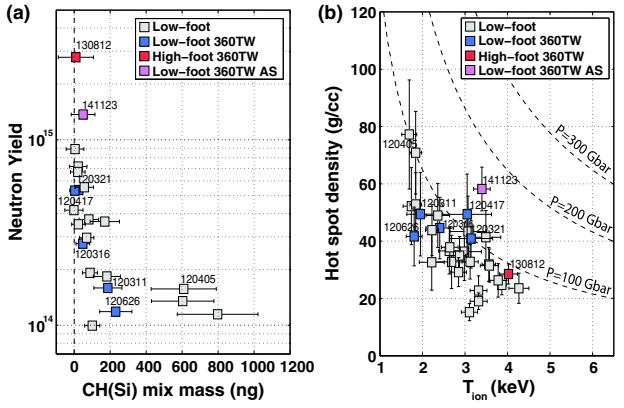

FIG. 4 (color online). (a) Total neutron yield plotted as a function of inferred CH mix mass. (b) Inferred hot spot density as a function of measured DT ion temperature. Plotted also are contours of inferred hot spot pressure. AS shot N141123 achieved considerable hot spot density and pressure compared to the comparable velocity LF and HF companions.

Figure 4(b) shows the inferred hot spot density as a function of the inferred ion temperature from the Doppler broadened DT neutron peak. Apparent in the plot is that the AS shot achieved higher hot spot temperature than the five comparable LF implosions along with higher hot spot density than the HF shot. Also included on the plot are contours of constant hot spot pressure. This high hot spot density and high temperature results in an inferred hot spot pressure of $P \sim 150$ Gbar for N141123, higher than any implosion during the NIC.

The performance variability of the low-foot companions is particularly striking. For example, N120321 holds the ITFX record during NIC for its combined yield and ρR [45], while its nearly identical companions (see Table I) achieved comparable ρR but with a range of observed yields and temperatures. Of particular note is shot N120311 (the closest companion to N141123 in terms of capsule dopant and hohlraum), which exhibited particularly low yield and temperature along with high inferred mix mass. No difference in initial condition has been identified that explains why N120311 performed much worse than N120321. It seems likely that these implosions were all near shell failure in flight and were especially sensitive to obscure perturbation sources such as the tent [44] or possible absorption of oxygen by the ablator [56]. The significantly lower yield of N120311 compared to the AS is related to the low observed Ti (~40%), a likely consequence of the high observed CH mix and accompanying radiative losses. Interestingly, the HF implosion achieved ~2X higher yield than the AS, but with reduced ρR [15], due to the higher adiabat. The increased yield is consistent with the 18% higher Ti. The picture that the LF design was near breakup is further supported by the fact that when the N120321-LF design was pushed to higher power (387 TW) and energy on shot N120405 (labeled gray point on Figs. 3 and 4), the performance was poor with a yield 1.6×10^{14} and with ~600 ng of CH mix into the hot spot. It is also noteworthy that the reduction of the ablation front growth on N141123 results in improved yield over LF implosions for which the inferred mix mass [Fig. 4(a)] was negligible, like N120321 and N120417 [45]. This suggests that even without mix of CH-ablator material into the hot spot, the feedthrough of ablation front growth to the hot spot boundary causes significant perturbation to the burning DT volume. This may also indicate that implosions during the NIC were significantly perturbed by ablation front growth even when the inferred CH mix was low or even negligible.

In summary, an "adiabat-shaped" indirect drive implosion designed to reduce ablation front growth and achieve high ρR has resulted in markedly improved performance when compared to the low-foot implosions during the NIC. This improvement suggests a dominant role of growth during the acceleration phase of the implosion in degrading implosion performance via reduced hot spot volume and

increased radiation losses from the mix of CH into the hot spot during the NIC. Recent results have shown that the tent perturbation [44], surface roughness, and other seeds internal to the plastic [56] are more severe than originally expected in ignition designs and have increased the relative role of the ablation front growth for implosions during the NIC. However, this result shows that these perturbations can be partly controlled using only the laser pulse shape while simultaneously achieving a high compression of $\rho R > 1$ g/cm^2. This represents an important step forward in managing the stability tradeoffs of achieving high velocity and high ρR, both necessary requirements for ignition.

The authors sincerely thank the NIF operations staff who supported this work. We gratefully acknowledge helpful conversations with O. Hurricane, J. Lindl, and J. Perkins. This work was performed under the auspices of the U.S. Department of Energy by Lawrence Livermore National Laboratory under Contract No. DE-AC52-07NA27344.

[1] E. I. Moses, J. Phys. Conf. Ser. **112**, 012003 (2008).
[2] J. D. Lindl, P. Amendt, R. L. Berger, S. G. Glendinning, S. H. Glenzer, S. W. Haan, R. L. Kauffman, O. L. Landen, and L. J. Suter, Phys. Plasmas **11**, 339 (2004).
[3] S. Atzeni and J. Meyer-ter-Vehn, *The Physics of Inertial Fusion*, International Series of Monographs on Physics (Oxford University Press, Oxford, 2004).
[4] J. P. Freidberg, *Plasma Physics and Fusion Energy* (Cambridge University Press, Cambridge, England, 2007).
[5] R. Betti, P. Y. Chang, B. K. Spears, K. S. Anderson, J. Edwards, M. Fatenejad, J. D. Lindl, R. L. McCrory, R. Nora, and D. Shvarts, Phys. Plasmas **17**, 058102 (2010).
[6] L. Rayleigh, *Scientific Papers II* (Cambridge University Press, Cambridge, England, 1900), p. 200.
[7] G. Taylor, Proc. R. Soc. A **201**, 192 (1950).
[8] R. Betti, V. N. Goncharov, R. L. McCrory, and C. P. Verdon, Phys. Plasmas **5**, 1446 (1998).
[9] A. J. Mackinnon *et al.*, Phys. Rev. Lett. **108**, 215005 (2012).
[10] S. P. Regan *et al.*, Phys. Rev. Lett. **111**, 045001 (2013).
[11] T. Ma *et al.*, Phys. Rev. Lett. **111**, 085004 (2013).
[12] M. J. Edwards *et al.*, Phys. Plasmas **20**, 070501 (2013).
[13] J. Lindl, O. Landen, J. Edwards, E. Moses, and N. Team, Phys. Plasmas **21**, 020501 (2014).
[14] T. R. Dittrich *et al.*, Phys. Rev. Lett. **112**, 055002 (2014).
[15] H. S. Park *et al.*, Phys. Rev. Lett. **112**, 055001 (2014).
[16] O. A. Hurricane *et al.*, Nature (London) **506**, 343 (2014).
[17] S. W. Haan *et al.*, Phys. Plasmas **18**, 051001 (2011).
[18] D. T. Casey *et al.*, Phys. Rev. E **90**, 011102 (2014).
[19] S. G. Glendinning *et al.*, Phys. Plasmas **7**, 2033 (2000).
[20] J. Milovich *et al.* preparation (to be published).
[21] D. S. Clark *et al.*, Phys. Plasmas **21**, 112705 (2014).
[22] M. M. Marinak, G. D. Kerbel, N. A. Gentile, O. Jones, D. Munro, S. Pollaine, T. R. Dittrich, and S. W. Haan, Phys. Plasmas **8**, 2275 (2001).
[23] K. L. Baker *et al.*, Phys. Plasmas **22**, 052702 (2015).
[24] K. O. Mikaelian, Phys. Rev. A **42**, 3400 (1990).
[25] A. L. Velikovich, F. L. Cochran, and J. Davis, Phys. Rev. Lett. **77**, 853 (1996).
[26] N. Metzler, A. L. Velikovich, and J. H. Gardner, Phys. Plasmas **6**, 3283 (1999).
[27] K. Anderson and R. Betti, Phys. Plasmas **10**, 4448 (2003).
[28] R. Betti, K. Anderson, J. Knauer, T. J. B. Collins, R. L. McCrory, P. W. McKenty, and S. Skupsky, Phys. Plasmas **12**, 042703 (2005).
[29] V. N. Goncharov, J. P. Knauer, P. W. McKenty, P. B. Radha, T. C. Sangster, S. Skupsky, R. Betti, R. L. McCrory, and D. D. Meyerhofer, Phys. Plasmas **10**, 1906 (2003).
[30] J. P. Knauer *et al.*, Phys. Plasmas **12**, 056306 (2005).
[31] V. A. Smalyuk, V. N. Goncharov, K. S. Anderson, R. Betti, R. S. Craxton, J. A. Delettrez, D. D. Meyerhofer, S. P. Regan, and T. C. Sangster, Phys. Plasmas **14**, 032702 (2007).
[32] R. D. Richtmyer, Commun. Pure Applied Math. **13**, 297 (1960).
[33] E. E. Meshkov, Izv. Acad. Sci. USSR Fluid Dyn. **4**, 101 (1969).
[34] V. N. Goncharov, Phys. Rev. Lett. **82**, 2091 (1999).
[35] J. L. Peterson, D. S. Clark, L. P. Masse, and L. J. Suter, Phys. Plasmas **21**, 092710 (2014).
[36] A. G. MacPhee *et al.* (to be published).
[37] J. L. Peterson, L. F. Berzak Hopkins, O. S. Jones, and D. S. Clark, Phys. Rev. E **91**, 031101 (2015).
[38] V. Smalyuk *et al.* (to be published).
[39] Note in some experiments with the LF, and HF pulses, a Au hohlraum with an additional 25 TW peak power was used to obtain a similar radiation drive, and, therefore, similar peak implosion velocities as DU (see Table I).
[40] T. Döppner *et al.*, Phys. Rev. Lett. **115**, 055001 (2015).
[41] Note here the hot spot radius is the effective radius inferred from the reconstructed x-ray volume.
[42] Note the values of $P * \tau$ are inferred from experimental data which are effected by alpha heating, while the motivating discussion in the introduction neglected alpha heating.
[43] D. S. Clark, S. W. Haan, B. A. Hammel, J. D. Salmonson, D. A. Callahan, and R. P. J. Town, Phys. Plasmas **17**, 052703 (2010).
[44] S. R. Nagel *et al.*, Phys. Plasmas **22**, 022704 (2015).
[45] V. A. Smalyuk *et al.*, Phys. Rev. Lett. **111**, 215001 (2013).
[46] P. Michel, W. Rozmus, E. A. Williams, L. Divol, R. L. Berger, S. H. Glenzer, and D. A. Callahan, Phys. Plasmas **20**, 056308 (2013).
[47] G. P. Grim *et al.*, Phys. Plasmas **20**, 056320 (2013).
[48] The outer contour is 17% of the peak with each inward contour increasing by integer multiples (17%, 34%, 51%, etc.).
[49] D. L. Bleuel *et al.*, Rev. Sci. Instrum. **83**, 10D313 (2012).
[50] J. R. Rygg *et al.*, Phys. Rev. Lett. **112**, 195001 (2014).
[51] A. L. Kritcher *et al.*, Phys. Plasmas **21** (2014).
[52] Note that here ρR is approximated from the measured neutron down-scattered ratio (DSR) where fuel $\rho R[g/\mathrm{cm}^2] \sim 0.19 \times \mathrm{DSR}$ [%] and total yield is inferred as $Y_{\mathrm{tot}} \sim Y_{13-15} e^{4.0*\mathrm{DSR}}$, where Y_{13-15} is the integrated neutron yield from 13–15 MeV.
[53] M. G. Johnson *et al.*, Rev. Sci. Instrum. **83**, 10D308 (2012).
[54] J. A. Frenje *et al.*, Nucl. Fusion **53**, 043014 (2013).
[55] P. Patel *et al.*, Bull. Am. Phys. Soc. **58**, 4.00001 (2013).
[56] S. W. Haan, H. Huang, M. A. Johnson, M. Stadermann, S. Baxamusa, S. Bhandarkar, D. S. Clark, V. Smalyuk, and H. F. Robey, Phys. Plasmas **22**, 032708 (2015).